$$\varphi(z) \cong (NZe^2 g\zeta / V c_l^2 k_c^2)\, z \ . \tag{22}$$

For c_l, the longitudinal sound velocity, the expression corresponding to a continuum with Young's modulus Y, Poisson's ratio σ, and mass density MN/v were used:

$$c_l^2 = \frac{Y(1-\sigma)}{(MN/v)(1+\sigma)(1-2\sigma)} \ . \tag{23}$$

The internal electric field is given by the gradient of $\varphi(z)$,

$$\vec{E}_{\rm int} = -\vec{\nabla}\left(\frac{1}{-e}\,\varphi(z)\right) = \frac{1}{e}\vec{\nabla}\varphi \ ,$$
$$\vec{E}_{\rm int} = \hat{z}\,\frac{N^2}{V^2}\,\frac{ZeMg}{k_c^2}\,\frac{(1+\sigma)(1-2\sigma)}{Y(1-\sigma)} \ . \tag{24}$$

Table I has some typical values of $\vec{E}_{\rm int}$.

Since the long-range phonons are mainly responsible for describing the gravitational compression of the lattice, perhaps a better value for ζ, the electron-phonon coupling constant, can be obtained from ultrasonic attenuation data than from resistivity data. The magnitude of the gravity-induced electric field is roughly an order of magnitude smaller than the values given in Table I, if ultrasonic data are used.

TABLE I. Typical values of $E_{\rm int}$.

Material	$E_{\rm int}$(V/m)
Cu	4.0×10^{-6}
Sn	6.2×10^{-6}
Pb	1.1×10^{-5}
Al	4.0×10^{-6}

ACKNOWLEDGMENT

The author would like to thank Dr. H. W. Lewis for suggesting the problem and for many helpful discussions.

†Work supported in part by the National Science Foundation.

[1]L. I. Schiff and M. V. Barnhill, Phys. Rev. 151, 1067 (1966).
[2]A. J. Dessler, F. C. Michel, H. E. Rorschach, and G. T. Trammell, Phys. Rev. 168, 737 (1968).
[3]C. Herring, Phys. Rev. 171, 1361 (1968).
[4]W. A. Harrison, Phys. Rev. 180, 1606 (1969).
[5]F. C. Witteborn and W. M. Fairbank, Phys. Rev. Letters 19, 1049 (1967).
[6]J. W. Beams, Phys. Rev. Letters 21, 1093 (1968).
[7]P. P. Craig, Phys. Rev. Letters 22, 700 (1969).
[8]M. Peshkin, Phys. Letters 29A, 181 (1969).
[9]A. A. Abrikosov, L. P. Gor'kov, and I. Y. Dzyaloshinskii, *Quantum Field Theoretic Methods in Statistical Physics* (Pergamon, New York, 1965), p. 76.

PHYSICAL REVIEW B VOLUME 2, NUMBER 4 15 AUGUST 1970

Equilibrium Defect Concentration in Crystalline Lithium

R. Feder
IBM *Research Division, Yorktown Heights, New York* 10598
(Received 11 August 1969)

The linear thermal expansion of pure lithium has been measured from 0 °C to the melting point by dilatometric and x-ray methods. Changes in length and lattice parameter were determined, respectively, by means of a Fizeau-type precision interferometer and by a high-angle backreflection x-ray technique. The two expansion curves diverge above 65 °C in a manner indicating the predominance of vacancy-type defects. If the divergence of the two curves is assumed to be due only to monovacancies, the results yield a formation energy $E_{1v}^f = 0.34 \pm 0.04$ eV and a formation entropy $S_{1v}^f = (0.9 \pm 0.8)k$. The value of E_{1v}^f accounts for 0.63 of the activation energy for self-diffusion. This result is much smaller than the corresponding ratio for Na, and, in fact, is comparable to results reported for fcc metals. The results are discussed in terms of the possible coexistence of monovacancies with either divacancies or interstitials.

I. INTRODUCTION

The x-ray dilatometric method employed in this work has previously been used to determine the equilibrium vacancy concentration in the following fcc metals: Ag,[1] Al,[2] Au,[3] Cu,[4] and Pb.[5] Although the vacancy concentration at the melting point varies between 1.7×10^{-4} and 9.4×10^{-4} (mole fraction),

the formation energy of a vacancy in this group of metals is almost a constant fraction of the activation energy for self-diffusion ($E_{1v}^f/Q \approx 0.57$). Furthermore, the entropy of formation for these fcc metals is approximately constant with a value between 1 and 2.

Extension of these types of measurements to metals other than fcc metals has only been reported so far on the bcc alkali metal Na.[6,7] The results reported in Ref. 6 indicate that for Na the vacancy formation energy accounts for almost the entire self-diffusion activation energy, with the ratio E_{1v}^f/Q being as high as 0.9. This result, which makes a striking contrast with the ratio for fcc metals, is in excellent agreement with recent calculations by Shyu *et al.*[8] A second noteworthy aspect of the results on sodium was the exceptionally large value reported for the entropy of formation ($S_{1v}^f/k = 5.8$), when compared to values obtained for the fcc metals. The high value for Na was explained in terms of the vacancy possessing a highly relaxed configuration, which is sometimes referred to as a relaxion. Such a configuration can be rationalized in terms of the high compressibility and more open structure of the alkali metals. Thus, it might be expected that, just as the fcc metals appear as a group to possess similar values of E_{1v}^f/Q and S_{1v}^f/k, the same may hold for the alkali metals. The purpose of the present work was to determine whether such conformability existed between sodium, and a second alkali metal, lithium.

A now familiar method of obtaining the equilibrium concentration of defects near the melting point involves a comparison of the x-ray thermal expansion as measured by the changes in lattice parameter and the bulk thermal expansion. The defect concentration, expressed as a mole fraction of lattice sites ($\Delta N/N$), is given at temperature T by the expression

$$\Delta N/N = 3(\Delta l/l_0 - \Delta a/a_0), \tag{1}$$

where l_0 and a_0 are the values of length and lattice parameter, respectively, at a low reference temperature, and Δl and Δa represent the corresponding changes in these quantities between the reference temperature and the temperature T. A negative or positive value of $\Delta N/N$ indicates the predominance of interstitials or vacancies, respectively. If a single species of defect is present, then the observed $\Delta N/N$ will be temperature dependent according to the following expression:

$$\Delta N/N = K \exp(S_d^f/k) \exp(-E_d^f/kT) , \tag{2}$$

where S_d^f and E_d^f are the entropy and enthalpy of formation, respectively, of the defect, K is a constant, k is Boltzmann's constant, and T is the absolute temperature. The magnitude of S_d^f, according to Huntington *et al.*,[9] will depend upon the type of defect present. For example, as the lattice relaxes about a vacant lattice site the vibrational frequencies decrease, thereby increasing the value of S_d^f. In the analysis of any experiment which determines the concentration of defects, consideration must be given to the possibility that more than one defect is present. For the present case, we will only be concerned with three types of defects, the monovacancy, the divacancy, and the interstitial. The equations relating the concentration of each defect with the entropy and enthalpy values are as follows:

For monovacancies,

$$C_{1v} = \exp(S_{1v}^f/k) \exp(-E_{1v}^f/kT); \tag{3}$$

and for divancies,

$$C_{2v} = 4 \exp(S_{2v}^f/k) \exp(-E_{2v}^f/kT), \tag{4}$$

where 4 is the number of distinguishable orientations of a divacancy in the bcc lattice.

For interstitials,

$$C_i = \exp(S_i^f/k) \exp(-E_i^f/kT) . \tag{5}$$

If E_{2v}^b is the binding energy of two vacancies to form a divacancy and S_{2v}^b is the binding entropy of a divacancy, then the energy and entropy of formation of a divacancy are given by

$$E_{2v}^f = 2E_{1v}^f - E_{2v}^b , \tag{6}$$

$$S_{2v}^f = 2S_{1v}^f - S_{2v}^b . \tag{7}$$

The simultaneous presence of these defects will produce a value of $\Delta N/N$ which is given by

$$\Delta N/N = C_{1v} + 2C_{2v} - C_i . \tag{8}$$

It should be noted from Eq. (8) that where more than one species of defect is present, the x-ray dilatometric measurements [Eq. (1)] yield only the *net* defect concentration. In such a case, the determination of the individual defect concentrations requires additional information, such as may be obtained, for example, from resistivity measurements. This will be discussed further in Sec. IV C.

II. EXPERIMENTAL METHOD

A. Specimen Preparation

A modified Bridgman technique was used to grow single crystals of high-purity zone-refined lithium in a grease-coated stainless steel mold. Since the density of lithium is less than the density of the liquefied apiezon grease used to protect the Li slugs from oxidation, it was necessary to grow the Li crystals from the top down. The mold, con-

sisting of three sections, followed the design of Nash and Smith.[10] The upper section provides a cavity of only $\frac{1}{16}$ in. diameter, which serves to produce a thin seed from which the larger crystal is grown. The mold assembly was placed on an adjustable pedestal which was inserted in a small tubular furnace which could be raised or lowered by a variable-speed motor. The entire apparatus was enveloped in an argon-filled plastic glove bag. The furnace was lowered at about 1 in./h. The yield of Li single crystals was almost 100%. The size of crystal obtained from the midsection of the mold was $\frac{3}{8}$ in. in diameter and 3 in. long. Removal was easily accomplished after the mold was separated into its three sections. The crystal was oriented on a goniometer table and made rigid by dipping the assembly into liquid paraffin. The orientation of the (420) plane was determined by the backreflection Laue technique. Satisfactory patterns were obtained only when the exposure was made with the x-ray tube held at about 10 kV and 20 mA, with an exposure time of about 4 h. Crystals were cut on a spark cutter into several disks 0.5 cm thick and one 5.2-cm rod, to provide the x-ray and dilatometer samples. The disk cuts were all made parallel to the (420) plane. The supporting paraffin was then removed from the disks, and these were then etched in methyl alcohol and stored in hexane to prevent oxidation.

The 5.2-cm-long cylindrical specimen was cleaned of all paraffin and immersed in light mineral oil. The ends were flattened and made parallel by compressing the sample to a length of 5 cm, using the jig previously described in the work on sodium.[6] The specimen was cleaned in hexane prior to insertion into the dilatometer. In handling the samples, it was observed that the oxidation rate of Li was much lower than that of Na. Fortunately, therefore, difficulties encountered with Na were not present with lithium. Specifically, no hysteresis was observed in the thermal expansion behavior. This will be discussed later in the paper.

B. X-Ray Method

The x-ray equipment used to measure the lattice parameter as a function of temperature is similar to that described in previous work.[6] The (420) crystal plane and Cu$K\alpha$ radiation provide a reasonably high-angle reflection. Over the temperature range from 0 to 180 °C, the corresponding Bragg angle varied from 79° to 77°, respectively. Because of the low values of the atomic scattering factor and the absorption coefficient for Li, the peak-to-background intensity ratio of the (420) reflection is relatively low. This necessitated comparatively long counting times during the step scanning operation over each peak. The counting time was increased with increasing temperature to give statistics such that the peak position of the reflection could be determined to within one part in 10^5.

C. Dilatometric Method

The changes in length as a function of temperature were measured using a Fizeau-type interferometer. The equipment used for this measurement has also been described previously.[6] A He-Ne laser is used as the light source and the fringes are counted automatically by a two-phototube system. The precision of measurement for a 5-cm specimen was approximately 1 ppm. A minor change in technique was necessitated by the use of a specimen in the form of a solid rod rather than a tube. In the present case, the upper optical flat was arranged to overhang the top surface of the specimen, so as to create a region at the side of the specimen for the appearance of the fringe pattern.

III. RESULTS

All thermal-expansion measurements of the x-ray lattice constant and the bulk crystal of Li were observed to be completely reversible during all heating and cooling cycles. This behavior contrasts with that of sodium, where exposure to air at room temperature for as little as 2 min causes the macroscopic thermal expansion to exhibit an irreversible behavior.[6] Dilatometric reversibility was only obtained with Na specimens which were carefully protected from oxidation. The absence of irreversibility for the Li samples is consistent with their noticeably lower oxidation rate. Expansion measurements were obtained from three separate specimens, and these are plotted versus temperature in Fig. 1 as the fractional change in length ($\Delta l/l_0$) and the fractional change in the lattice constant ($\Delta a/a_0$). The lattice constant and length measurements were made from 0 to 179 °C. Smooth curves were drawn through the $\Delta l/l_0$ points and $\Delta a/a_0$, respectively. The lower-temperature scale and the right-hand ($\Delta l/l_0$), ($\Delta a/a_0$) scales refer to the lower curves. The upper-temperature scale and left-hand ($\Delta l/l_0$), ($\Delta a/a_0$) scales belong to the upper set of curves. The two expansion curves coincide from 0 to about 65 °C and subsequently diverge. For convenience, the two sets of measurements were pinned at 20 °C. The absolute value of the lattice parameter at 20 °C was obtained by averaging over five specimens and found to be 3.50914 Å. This compares favorably with the lattice constant given in the International Tables[10a] (a_{20} = 3.5092 Å). The data points obtained from the length measurements represent results from runs on three specimens. The circular symbols represent the dilatometric thermal expansion and the

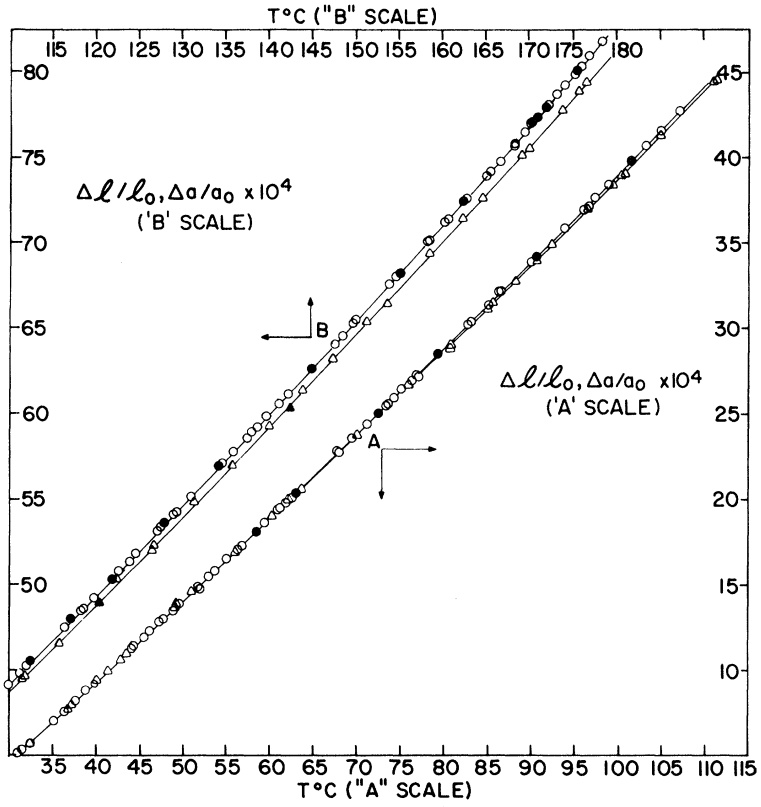

FIG. 1. Length and lattice-parameter expansion of lithium versus temperature. Curves A (31–110 °C) are represented by lower and right-hand scales; curves B by left and upper scales. Circles represent length changes while triangles represent lattice parameter changes. Open symbols are used for heating runs and filled symbols for cooling runs.

triangles represent the thermal expansion as measured by changes in the x-ray lattice parameter. Open symbols denote results of heating, whereas the solid symbols denote values on cooling. In Fig. 1, the maximum deviation of any experimental point from the corresponding drawn curve is 1×10^{-5}. The difference between the two curves $(\Delta l/l_0 - \Delta a/a_0)$ is 1.47×10^{-4} at the melting point. Thus, from Eq. (8), the corresponding net defect concentration $\Delta N/N$ is 4.4×10^{-4}.

The data points for $\Delta a/a$ do not, in general, fall at the same temperatures as those for $\Delta l/l_0$. Also, as was previously mentioned, the precision of $\Delta l/l_0$ is much greater than that of $\Delta a/a_0$. Consequently, $\Delta N/N$ was determined as a function of temperature by taking the difference between the x-ray experimental points and the smooth curve for the macroscopic expansion. Figure 2 shows this difference in a semilogarithmic plot of $\Delta N/N$ as a function of the reciprocal temperature. Whenever several x-ray measurements were made at a given temperature, these values were averaged. The vertical bars in Fig. 2 show the average error for each point, which is 1 part in 10^5. Although bars are shown for only a few of the data points, this error applies to all of the points. The solid line is the best straight line that could be drawn through the data points. Although a straight line was drawn through the data points, it is conceivable that a curve could have been drawn through the points with a slight negative curvature. With one exception, all points are within 3 parts in 10^5 of the drawn line. The values derived from the experimental slope and intercept of Fig. 2 will be defined as an "effective" formation energy E^f and entropy of formation S^f. Only when a single defect exists can E^f be set equal to E_d^f and S^f to S_d^f. From Fig. 2, we obtained the value of $E^f = 0.34 \pm 0.04$ eV from the slope of the curve and $S^f/k = 0.9 \pm 0.8$ eu from the intercept of $1/T = 0$.

IV. DISCUSSION

It can be seen from Fig. 1 that once the $\Delta l/l$ and $\Delta a/a$ curves diverge $\Delta l/l$ is always greater at any given temperature. Hence, the positive value of $\Delta N/N = 3(\Delta l/l - \Delta a/a)$ shows that the predominant defect in thermodynamic equilibrium at elevated temperatures is of the vacancy type. Furthermore, the difference between the curves plotted in Fig. 2 indicates that, within experimental error, the defect concentration varies exponentially with $1/T$. This is consistent with the presence of a single-defect species.

As shown in Table I, a comparison of the values of E^f and S^f/k reported for Na and the present experimental values for Li reveal that, despite the

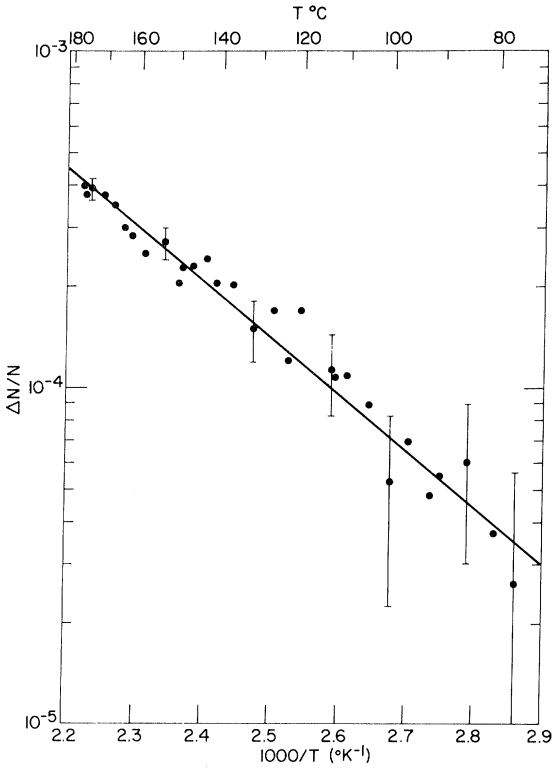

FIG. 2. Semilogarithmic plot of net-defect concentration versus reciprocal temperature. Bars represent average error for each datum point.

higher melting point, E^f (Li) is less than E^f (Na). Also, S^f/k (Li) is appreciably less than S^f/k (Na). In terms of these parameters, Li is quite different from Na. An analysis of the results on Na indicate quite strongly that the vacancy was the major defect present, so that E^f (Na) $= E^f_{1v}$ (Na) and S^f/k (Na) $= S^f_{1v}/k$ (Na). Accordingly, we shall first examine the consequences of a similar assignment for Li. Following this, consideration will be given the results in terms of the coexistence of vacancies with other species of defects.

A. Monovacancies

If we assume that the defect concentration (Fig. 2) is due only to single vacancies, we have the vacancy-formation energy (E^f_{1v}) from the slope and the entropy of formation (S^f_{1v}) from the intercept of the curve at $1/T = 0$. This gives a value of 0.34 eV for the formation energy and 0.9 eu for the entropy of formation. If we use the average value $Q = 0.54 \pm 0.04$ for the self-diffusion activation energies reported by Ailion and Slichter[11] and Hultsch and Barnes,[12] the ratio E^f_{1v}/Q is found to be 0.63. This value is somewhat greater than the ratio found for fcc metals, and substantially less than the value $E^f_{1v}/Q = 0.9$ found for bcc sodium. If we subtract the present value of E^f_{1v} from the value of Q we obtain a value of 0.20 ± 0.06 eV for the activation energy for vacancy motion E^m_{1v}. The best values to date of the principal parameters for Li and Na are listed in Table I.

It is somewhat surprising that the two alkali metals are not more similar in the values of E^f given in Table I. It can be seen from Table I that the values of Q for Li and Na correlate in the expected way with their melting points, and the same behavior could have been expected for E^f_{1v}. However, our results show that despite this expectation the formation energy E^f_{1v} (Li) $< E^f_{1v}$ (Na). The only experimental comparison that can be made with the present result is the excess resistivity measurement of MacDonald[13] who reported a formation energy of 0.40 ± 0.02 eV. Even though this result is somewhat higher than ours, there is agreement within experimental error. MacDonald's findings again point to the conclusion that $(E^f/Q)_{\mathrm{Li}} < (E^f/Q)_{\mathrm{Na}}$. The present results may also be compared with the theoretical calculations of Kojima,[14] McClellan[15] and Fumi.[16] Kojima applied a correction to a Huntington-Seitz-type calculation and found $E^f_{1v} = 0.4$ eV. McClellan obtained a value of $E^f_{1v} = 0.33$ eV from a strain energy calculation. Fumi, calculating the changes in potential upon the creation of a vacancy, obtained $E^f_{1v} = 0.55$ eV. If one uses a simplified shear-strain energy approach for Li as proposed by Lazarus,[17] the vacancy-motion energy for Li would be $E^m_{1v} = 0.28$ eV, implying that $E^f_{1v} = 0.26$ eV. Except for the calculation made by Fumi, the other calculations are consistent with the assignment of the result $E^f = 0.34$ eV as the vacancy-formation energy. The weight of theoretical evidence apparently supports the view that E^f (Li) $< E^f$ (Na).

A comparison of the S^f/k values for Li and Na again reveals significant differences between the two metals. A high value of S^f/k as found for Na is usually taken as indicative of a highly relaxed vacancy configuration. This could have been expected for Li but surprisingly is not the case. The relatively low values of S^f/k and E^f/k for Li make it look much more like a fcc metal. The unexpected low value of S^f/k for Li is an apparent contra-

TABLE I. Principal parameters for Li and Na.

	Li	Na
Q(eV)	0.54 ± 0.02 (Refs. 11 and 12)	0.445 ± 0.015 (Ref. 19)
S/k	2.0	3.5 ±0.7
E^f (eV) observed	0.34 ± 0.04	0.42 ± 0.03
S^f/k observed	0.9 ±0.8	5.8 ±1.1
E^m (eV)	0.19	0.04

diction to the results of pressure experiments on self-diffusion by Hultsch and Barnes.[12] These investigators found that a pressure of 7000 atm reduced the self-diffusion coefficient in Li by a factor of 3, whereas a pressure of 3000 atm reduced the self-diffusion coefficient in Na by a factor of 6. From measurements of this type, the activation volume ratio $\Delta V/V_a$ was found to be 0.28 for Li and 0.41 for Na, which indicates that the relaxation about a vacancy is even larger in Li than it is in Na.[18] It might have been expected, therefore, that S^f/k for Li should have been even larger than the value for Na. This explicitly is not the case. The cause of this anomaly may reside in the assumption that S^f/k monotonically increases as the relaxation becomes progressively larger. In one respect, the concept that the vacancy in Li is even more highly relaxed than in Na does appear to be consistent with the present findings. As Hultsch and Barnes have pointed out, the energy for an atom to jump into a vacancy may increase as the relaxation becomes larger. This implied that E^m_{1v} for Li should be greater than for Na, in accord with the present interpretation.

In summary, starting with the assumption that monovacancies are the only defect species present, we must conclude that the parameters characterizing the vacancy concentration in Li resemble those for the noble fcc metals more closely than they do for Na. In the remainder of the discussion, we shall attempt to see how this conclusion can be modified by considering the coexistence of monovacancies with other defects. In view of the sharp contrast between the present results on Li and those previously reported for Na, we have sought in particular to find schemes for which E^f_{1v} and S^f_{1v} would assume higher values.

B. Coexistence of Monovacancies and Divacancies

For this situation, Eq. (8) reduces to $\Delta N/N = C_{1v} + 2C_{2v}$. From this expression, we can conclude that the exponentials for C_{1v} and C_{2v} must be below the $\Delta N/N$ curve at all temperatures. If we then require that $E^f_{1v} > E^f$, we must assume that $E^f_{2v} < E^f_{1v}$. This is in itself a most unlikely situation. Furthermore, even if this condition is assumed, highly unrealistic values of S^f_{2v} are required to obtain the required fit to the $\Delta N/N$ plot. We may conclude, therefore, that coexistence with divacancies cannot serve to explain the difference in the E^f and S^f/k values between Li and Na.

C. Coexistence of Monovacancies and Interstitials

The expression to cover the coexistence of monovacancies and interstitials for the present type of measurement is $\Delta N/N = C_v - C_i$. In contrast, it should be noted that in a resistivity type of measurement, such as performed by MacDonald,[13] the net resistivity change $\Delta p/p$ would be the sum of terms $AC_v + BC_i$, where the constants A and B give the resistivity change per unit concentration of defects. With this in mind an attempt has been made to compare MacDonald's data with the present results. To do so, the following assumptions were made: (a) The constants A and B were assumed equal; (b) the total defect concentration in Li at its melting point was taken to be roughly the same as that for Na at its melting point. With these assumptions, MacDonald's data can be transformed to the plot marked $(C_v + C_i)$ in Fig. 3, for comparison with the $\Delta N/N$ curve (which is now regarded as the $C_v - C_i$ curve). Using these two curves we obtain the curves for C_v and C_i separately as shown in Fig. 3. From these we obtain the values of $E^f_{1v} = 0.37$ eV, $S^f_{1v} = 2.0$ and $E^f_i = 0.47$ eV, $S^f_i/k = 3.1$. The reason that this new estimate of E^f_{1v} is not appreciably higher than the E^f value of Table I is that this value of E^f is only slightly smaller than the E^f value obtained by MacDonald (0.4 eV). In fact, it appears that the relatively small difference between these values of E^f can be even further reduced by drawing a different

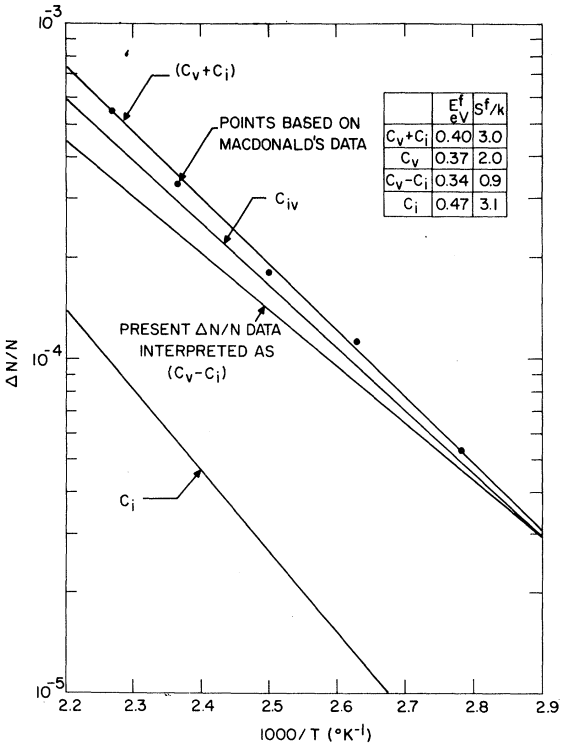

FIG. 3. Combined analysis of MacDonald's resistivity data and the present $\Delta N/N$ data, according to the assumptions made in the text.

line through MacDonald's data to give less weight to the uppermost data point. Thus, the evidence suggests that E^f cannot be greatly different from E^f_{1v}. This conclusion was reinforced by performing graphical exercises in which attempts were made to force E^f_{1v} and S^f_{1v}/k to higher values, such that $S^f_{1v}/k \approx 5$ and E^f_{1v}/Q has the value 0.9 found for Na. While such self-consistent analysis can be performed (and indeed yield the slight negative curvature exhibited by the data points in Fig. 2), the required entropy factors for the interstitial are so large and positive ($S^f_i/k \approx 9$) that the realism of such constructions is open to considerable doubt.

V. CONCLUSIONS

It is clear that the vacancies are the predominant defect in Li, as they are in Na. However, the values for E^f and S^f/k for these metals are not similar. Attempts to explain the differences in terms of coexistence of vacancies with other defects have not been successful and, in fact, serve to reinforce the view that E^f_{1v} for Li cannot be greatly different from the measured value E^f = 0.34 eV. Though this is significantly smaller than the value found for Na (0.42 eV), this result appears to be consistent with MacDonald's measurements and with the tenor of theoretical calculations. As a corollary, it appears, therefore, that the migration of a vacancy in Li is appreciably higher than in Na. Perhaps the most surprising single result of this work is the finding that the vacancy entropy factor in Li is of comparable value to those found for the noble metals, since the work of Hultsch and Barnes gives strong evidence that the vacancy configuration in Li is very highly relaxed. This result suggests that new theoretical calculations to obtain the entropy factor for various large degrees of relaxation would be of value.

ACKNOWLEDGMENTS

The author would like to thank D. Gupta for stimulating discussions and B. S. Berry for critically reviewing the manuscript. This work was supported in part by the U. S. Atomic Energy Commission.

[1]R. O. Simmons and R. W. Bulluffi, Phys. Rev. 119, 600 (1960).
[2]R. O. Simmons and R. W. Bulluffi, Phys. Rev. 117, 52 (1960).
[3]R. O. Simmons and R. W. Bulluffi, Phys. Rev. 125, 862 (1962).
[4]R. O. Simmons and R. W. Bulluffi, Phys. Rev. 129, 1533 (1963).
[5]R. Feder and A. S. Nowick, Phil. Mag. 15, 805 (1967).
[6]R. Feder and H. Charbnau, Phys. Rev. 149, 464 (1966).
[7]G. A. Sullivan and J. W. Weymouth, Phys. Rev. 136, A1141 (1964).
[8]W. -M. Shyu, D. Brust, and F. G. Fumi, J. Phys. Chem. Solids 28, 717 (1967).
[9]H. B. Huntington, G. A. Shien, and E. S. Wajda, Phys Rev. 99, 1085 (1955).
[10]H. C. Nash and C. S. Smith, J. Phys. Chem. Solids 9, 113 (1959).
[10a]*International Tables for X-Ray Crystallography* (The Kynoch Press, Birmingham, England, 1962), Vol. III, p. 279.
[11]D. C. Ailion and C. P. Slichter, Phys. Rev. 137, A235 (1965).
[12]R. A. Hultsch and R. G. Barnes, Phys. Rev. 125, 1832 (1962); D. F. Holcomb and R. E. Norberg, *ibid.* 98, 1074 (1955).
[13]D. K. C. MacDonald, J. Chem. Phys. 21, 177 (1953).
[14]T. Kojima, J. Phys. Soc. Japan 11, 717 (1956).
[15]R. B. McClellan (private communication).
[16]F. G. Fumi, Phil. Mag. 46, 1007 (1955).
[17]D. Lazarus, Phys. Rev. 93, 973 (1954).
[18]It is worth noting that even though the relaxation around a vacancy is larger in Li than in Na, the compressibility of Na is 50% greater than that of Li.
[19]N. H. Nachtrieb, E. Catalano, and J. A. Weil, J. Chem. Phys. 20, 1185 (1952).